Nuclear Inst, and Methods in Physics Research B 432 (2018) 48–54

Contents lists available at ScienceDirect

Nuclear Inst. and Methods in Physics Research B

journal homepage: www.elsevier.com/locate/nimb

Electrical and structural characterization of neutron irradiated amorphous boron carbide/silicon p-n heterojunctions

Michael Nastasi[a,b,c,*], George Peterson[a], Qing Su[b], Yongqiang Wang[d], N.J. Ianno[c,e], Nicole Benker[f], Elena Echeverría[f], Andrew J. Yost[f], J.A. Kelber[g], Bin Dong[g], Peter A. Dowben[c,f]

[a] Department of Mechanical and Materials Engineering, University of Nebraska, Lincoln, NE 68588-0526, United States
[b] Nebraska Center for Energy Sciences Research, University of Nebraska, Lincoln, NE 68583-0857, United States
[c] Nebraska Center for Materials and Nanoscience, University of Nebraska, Lincoln, NE 68588-0298, United States
[d] Materials Science and Technology Division, Los Alamos National Laboratory, Los Alamos, NM 87545, United States
[e] Department of Electrical and Computer Engineering, University of Nebraska, Lincoln, NE 68588-0511, United States
[f] Department of Physics and Astronomy, University of Nebraska, Lincoln, NE 68588-0299, United States
[g] Department of Chemistry, 1155 Union Circle #305070, University of North Texas, Denton, TX 76203, United States

ARTICLE INFO

Keywords:
Semiconducting boron carbides
Hydrogenated boron carbides
Radiation hardness
Neutron irradiation
Neutron detectors
Neutron voltaics

ABSTRACT

The electrical and structural properties of amorphous hydrogenated semiconducting boron carbide on silicon p-n heterojunction diodes have been examined following irradiation with thermal neutrons to a maximum dose of 1.08×10^9 neutrons/cm^2. Improvements in the current-voltage response of the heterojunction diode, along with a decrease in the diode ideality factor, are observed with neutron exposure. Capacitance-voltage data were used to extract the hydrogenated boron carbide carrier density and diode built-in potential, both of which decrease with irradiation. Structural and defect characterization, carried out with high resolution TEM and RBS in channeling mode, show that the hydrogenated boron carbide remains amorphous and no discernible damage occurs in the Si component of the diode. These data suggest that the observed changes in electrical properties result from irradiation induced defect passivation in the amorphous boron carbide. For n-type plasma enhanced chemical vapor deposition hydrogenated semiconducting boron carbide on p-type silicon, the improvements in the heterojunction diode are quite dramatic.

1. Introduction

Semiconducting boron carbide/silicon diodes have been investigated for some time for applications as a solid-state neutron detector [1–8] (for a review see [3]) and as a potential energy source as a neutron voltaic [7,8]. Both applications are derived from the interaction of thermal neutrons with ^{10}B, which has a capture cross section of 3840 ± 0.016 barns [3]. ^{10}B neutron capture leads to the loss of boron and creation of daughter fragments with significant kinetic energy [9]. The primary reaction products are the production of 0.84 MeV ^{7}Li and 1.47 MeV ^{4}He ions. Following the capture/fragmentation process, the ^{7}Li and ^{4}He ions deposit energy as they traverse the device in the form of electronic excitation and ionizing (electronic energy deposition) or elastic displacement collisions (nuclear energy deposition) [10]. The deposited ionizing energy creates electron-hole pairs along the ion tracks, and the electric field created across the diode junction separates the charges, generating a current pulse. While this phenomena has been well documented, little previous work has been done to examine the resulting radiation damage effects on the electrical performance of the boron carbide/silicon diode.

Our previous study [11] used 200 keV He ions to simulate alpha particles generated by the neutron capture and fragmentation process in boron carbide/silicon p-n junctions. These studies [11] showed that electrical performance initially improved under irradiation and that higher irradiation doses led to device failure as a result of nuclear damage in the crystalline silicon substrate. It was hypothesized that initial device improvement resulted from electronic energy deposition in the amorphous boron carbide, which resulted in bond breaking and reformation, thereby removing bond defects (defect passivation) that resulted during synthesis. In this work, we use thermal neutrons as the irradiating source, where high energy fragments are produced from neutron capture by a ^{10}B atom in the boron carbide film, to further our understanding of irradiation effects on amorphous boron carbide/Si devices. Our aim is to provide additional insight into the changes of the

* Corresponding author at: Department of Mechanical and Materials Engineering, University of Nebraska, Lincoln, NE 68588-0526, United States.
E-mail address: mnastasi2@unl.edu (M. Nastasi).

https://doi.org/10.1016/j.nimb.2018.07.006
Received 3 May 2018; Received in revised form 2 July 2018; Accepted 2 July 2018

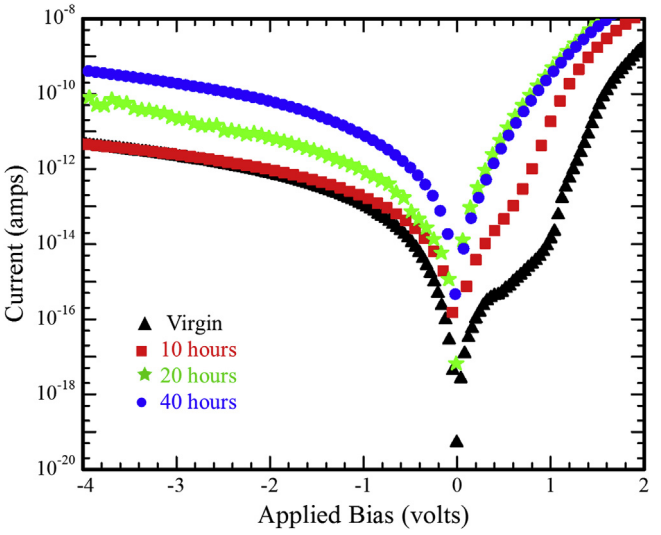

Fig. 1. The current versus voltage curves of a p-n diode following neutron irradiation fluences of zero, 2.7×10^8, 5.4×10^8, and 10.8×10^8 neutrons/cm^2; i.e. 0 (virgin), 10, 20, and 40 h of exposure, respectively.

device as a result of neutron irradiation induced changes in the amorphous partially dehydrogenated semiconducting boron carbide.

2. Experimental details

The plasma enhanced chemical vapor deposition (PECVD) hydrogenated semiconducting boron carbide, $B_{10}C_{2+x}H_y$, based p-n heterojunction were synthesized using an n-type silicon (P doped) substrate (0 0 1) of resistivity 65−110Ω × *cm* (University Wafers). The substrates were cleaned in baths of acetone, methanol, and filtered de-ionized water followed by a 5 wt% hydrofluoric acid (HF) bath for oxide removal and hydrogen termination. Prior to a-$B_{10}C_{2+x}H_y$ deposition, the substrate was exposed to a 30 min Ar^+ plasma etch to remove any residual carbon or other surface impurities. Partially dehydrogenated boron carbide thin films were deposited on the Si via plasma enhanced chemical vapor deposition (PECVD) utilizing ortho-carborane (*closo*-1,2 dicarbadodecaborane, $C_2B_{10}H_{12}$) (Sigma Aldrich) as the source compound at 350 °C. Details of the deposition process have been previously reported [1,4,12]. The composition of the deposited a-$B_{10}C_{2+x}H_y$ films was established by elastic recoil detection measurements [11], with x approximately equal to 0 and y approximately equal to 4. The n-type boron carbide heterojunctions were formed by plasma enhanced chemical vapor deposition (PECVD), as described in prior work [2,13], using *closo*-1,7-dicarbadodecaborane (metacarborane, m-$B_{10}C_2H_{12}$) in a 20 mTorr Ar inductively coupled plasma (20 W), and deposited on atomically clean p-type Si(1 0 0).

In this report, diodes consisting of films derived from PECVD of orthocarborane on n-type Si are referred to as p-n devices. Conversely, diodes consisting of PECVD metacarborane films on p-type Si are labelled as n-p devices.

Contact metallization consisting of Cr, with a Au capping layer was deposited on the p-n heterojunction through a d.c. magnetron sputter source (AJA International Inc.) at a base pressure below 1×10^{-7} Torr. Both metals were sputtered in an Ar^+ plasma at a pressure of 5 mTorr to a thickness of approximately 300 nm.

Neutron irradiation of the heterojunction p-n diodes was carried out using a deuterium-tritium (D-T) neutron source (Thermo Scientific MP 320 neutron generator). The output of the D-T source is 14 MeV neutrons, which was combined with a 10 cm beryllium (Be) cube neutron multiplier. The neutrons were moderated by 1 in. of paraffin, providing approximately 7500 neutrons/cm^2/s with a slightly anisotropic 4π neutron environment for the irradiated samples. Further details

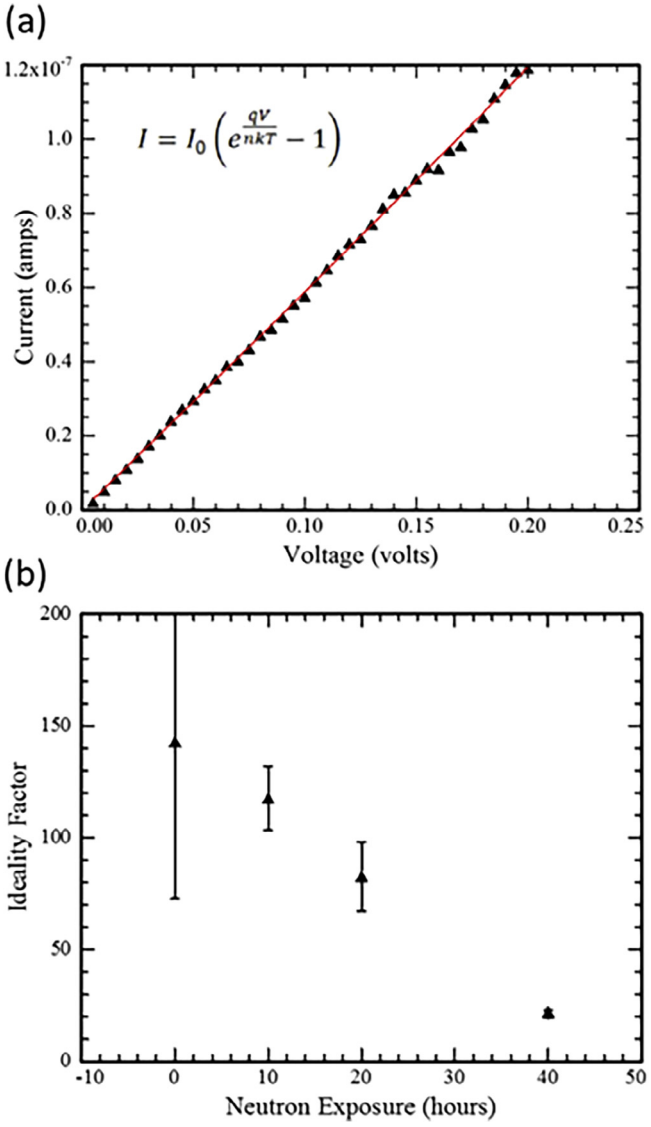

Fig. 2. (a) shows the fitting results (red line) of Eq. (1) (insert in (a)) to the p-n diode current–voltage data to obtain the ideality factor of current due to thermal recombination of carriers in the depletion region. (b) shows the ideality factor as a function of neutron exposure. Neutron fluences of zero, 2.7×10^8, 5.4×10^8, and 10.8×10^8 neutrons/cm^2 correspond to 0, 10, 20, and 40 h of exposure, respectively. (For interpretation of the references to colour in this figure legend, the reader is referred to the web version of this article.)

about the neutron source can be obtained elsewhere [5,6]. Neutron moderation was confirmed by exposing single crystal Si to 10.8×10^8 neutrons/cm^2 followed by ion channeling where no damage build up was observed. Diode samples were exposed to the neutron flux for 10, 20, and 40 h resulting in neutron fluences of 2.7×10^8, 5.4×10^8, and 10.8×10^8 neutrons/cm^2, respectively.

The number of neutron reactions with ^{10}B was calculated following Hoglund et. al. [14], assuming a film composition of $B_5C_1H_2$ (determined by elastic recoil detection analysis), a film thickness of 300 nm, a mass density of 1.7 g/cm^3 (determined by x-ray reflectivity), and a reaction cross-section of 3840 barns. The fraction of ^{10}B was taken as 20% of the boron fraction. This analysis indicates that 0.173% of the thermal neutrons were absorbed by ^{10}B, resulting in the production of 1.86×10^6 (α + Li)/cm^2 for a 10.8×10^8 neutrons/cm^2 exposure.

Structural characterization of the p-n device before and after neutron irradiation was performed using high resolution transmission

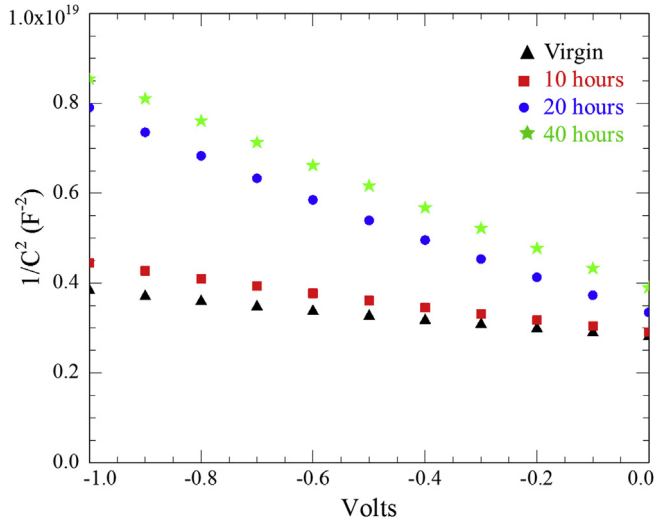

Fig. 3. Data shows the linear relationship between $1/C^2$ and the applied voltage as a function of neutron exposure for the p-n diode. The data are plotted for neutron fluences of zero, 2.7×10^8, 5.4×10^8, and 10.8×10^8 neutrons/cm^2; i.e. 0 (vigin), 10, 20, and 40 h of exposure, respectively.

electron microscopy (HRTEM), selected area electron diffraction (SAED) and Rutherford backscattering spectrometry (RBS) in channeling mode (RBS/C). Cross-sectional TEM specimens were prepared by conventional dimple and grinding followed by ion-milling. Low energy (3.5 keV) and low angle (5°) were selected to reduce the ion milling damage. A FEI Tecnai G2 F20 TEM was used to investigate the microstructure of these films. Ion channeling experiments were carried out at the Center for Integrated Nanotechnologies (CINT), within Los Alamos National Laboratory (LANL), using a 3MV tandem accelerator with 2 MeV ^{4}He + ions in the Cornell scattering geometry with the detector at 167°.

Current versus voltage measurements were obtained using a Keithley 2411B SourceMeter to deliver a dc voltage, a Keithley 6485 PicoAmmeter to measure the resulting current, and a HP 3478A Multimeter to measure the voltage across the device under test. Capacitance versus voltage measurements were obtained using an HP model 4192A impedance analyzer with an oscillation voltage set to 0.010 V in a 4-point parallel circuit.

3. Results and discussion

The current versus voltage curves of a p-n diode following neutron irradiation fluences of zero, 2.7×10^8, 5.4×10^8, and 10.8×10^8 neutrons/cm^2; i.e. 0 (virgin), 10, 20, and 40 h of exposure, respectively are seen in Fig. 1. What is immediately apparent in Fig. 1 is that the forward bias region of the *I(V)* curve in the virgin measurement (measurements prior to neutron fluence exposure, as in Fig. 1) shows structure between 0 and 0.5 V that diminishes after 2.7×10^8 neutrons/cm^2 (10 h) of irradiation and disappears after 5.4×10^8 neutrons/cm^2 (20 h) of irradiation. This may be due to a heterogenous mixture of trapping states in PECVD hydrogenated boron carbide, especially midgap states [15], as well as a multiplicity of contributions to the carrier concentration. Also, it is evident that after 10 h of irradiation, corresponding to roughly 2.7×10^8 neutrons/cm^2, the forward diode current increases for all forward voltages, while the reverse bias current remains approximately constant. In general this would be considered improved diode performance. Beyond 10 h of exposure, both the forward and reverse currents increase, and at 40 h of exposure (10.8×10^8 neutrons/cm^2) the reverse current at −2V is only 2 orders of magnitude lower the forward current at 2 V.

A simple diode current-voltage relationship is given in Eq. (1): [16]

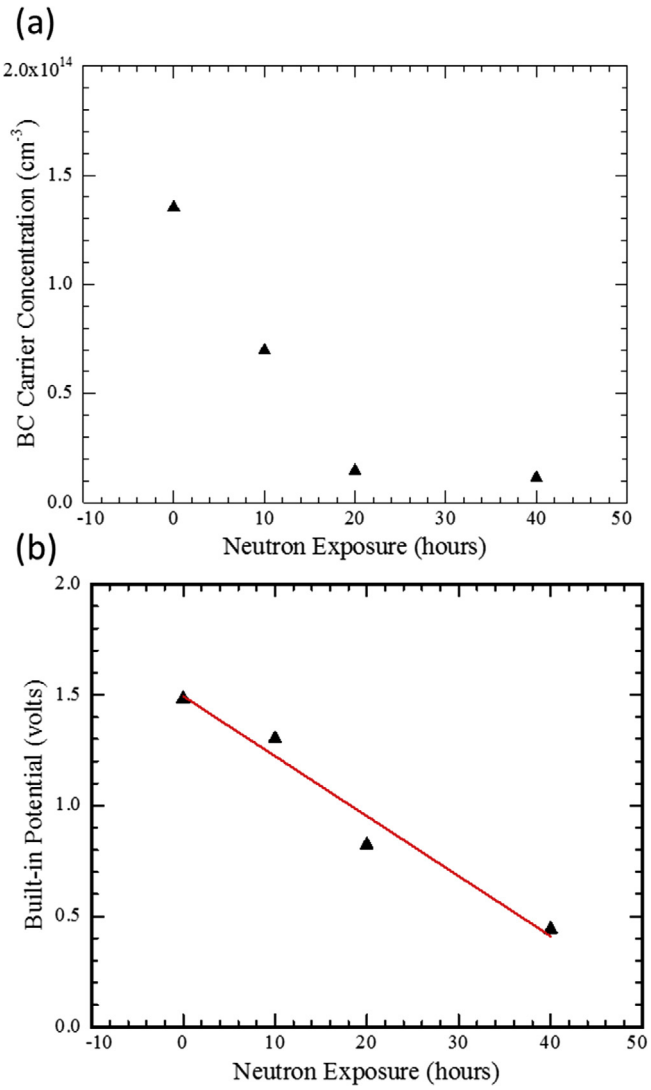

Fig. 4. The amorphous-$B_{10}C_{2+x}H_y$ carrier density in the p-n diode as a function of neutron exposure (a), and the built-in potential as a function of neutron exposure (b). Neutron fluences of zero, 2.7×10^8, 5.4×10^8, and 10.8×10^8 neutrons/cm^2 correspond to 0, 10, 20, and 40 h of exposure, respectively. The solid trace in (b) is a least-squares fit to the data. Note: Error bars are ≤ symbol size.

$$I = I_0\left(e^{\frac{qV}{nkT}} - 1\right) \quad (1)$$

where I is the net current flowing through the diode, I_o is the dark saturation current, V is the applied voltage, q is the value of electron charge, k is Boltzmann's constant, T is the absolute temperature, and n is the ideality factor. This equation results from a combination of the ideal diode model and recombination-generation in the depletion region, where the ideality factor is a measure of how closely the diode follows the ideal diode equation; in an ideal diode, n = 1. Fig. 2 shows the results of fitting the data in Fig. 1 to Eq. (1) over the voltage range 0–0.25 V (Fig. 2a) to obtain the ideality factor as a function of neutron exposure (Fig. 2b).

As Fig. 2b shows, the ideality factor is well beyond the upper limit of 2 in all cases, which suggests the simple model of an ideal diode plus R-G in the depletion region is inadequate to model the device. However, the effect of the thermal neutron radiation is quite clear. The fit to Eq. (1) linearly improves with exposure, although it is unknown whether exposure beyond 10.8×10^8 neutrons/cm^2 will ultimately reduce n to 2 or below. While these results show the effect of thermal neutrons on

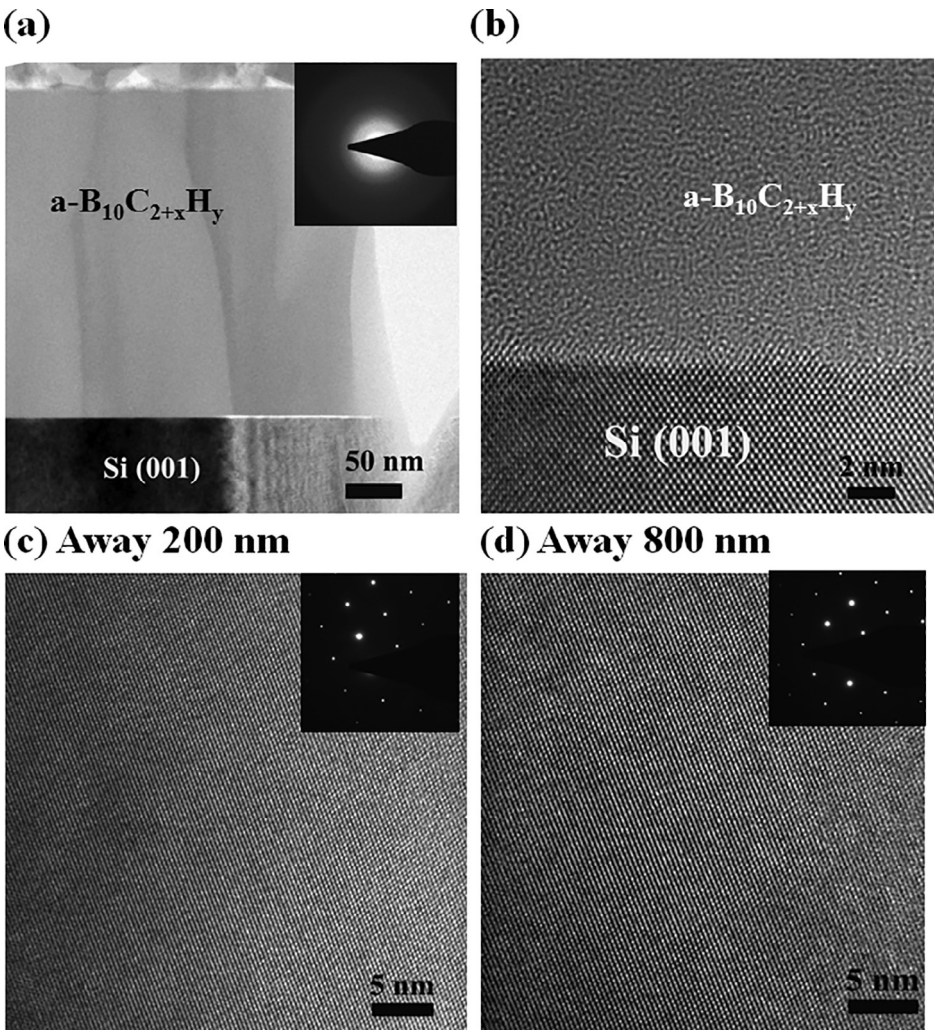

Fig. 5. All TEM data presented were take following 40 h of neutron exposure (10.8×10^8 neutrons/cm^2). (a) Low magnification TEM image of the a-$B_{10}C_{2+x}H_y$/Si (p-n diode) interface with the inset showing the SAED pattern from the a-$B_{10}C_{2+x}H_y$, composed of halos indicative of the amorphous structure. (b) the HRTEM image shows that the Si substrate remains crystalline near the junction interface and that the junction interface remains abrupt. HRTEM images of (c) 200 nm and (d) 800 nm away from the interface, no indication of defect formation is observed.

diode properties, they do not provide a clear mechanism responsible for the observed changes.

In view of this the p-n diode capacitance–voltage response was studied. The junction capacitance per unit area of an ideal, abrupt heterojunction diode can be described by [17]:

$$C = \left(\frac{q \in_n \in_p N_a N_d}{2(\in_p N_a + \in_n N_d)} \right)^{1/2} (V_i - V_a)^{-1/2} \quad (2)$$

where q is the electronic charge, ε_n and ε_p are the permittivity for Si and amorphous-$B_{10}C_{2+x}H_y$, respectively, N_a and N_d are the doping densities of amorphous-$B_{10}C_{2+x}H_y$ and Si, respectively, V_i is the built-in potential, and V_a is the applied voltage. By rearranging Eq. (2) in the form of $1/C^2$, this leads to a relationship that is linear with V_a. Fig. 3 shows the diode obeys the linear relationship between $1/C^2$ and V_a as a function of neutron exposure, which allows the extraction of meaningful date from this diode model. The data show that the slope increases with increasing neutron fluences, while the capacitance decreases.

Assuming that the only changes taking place during neutron irradiation are occurring in amorphous hydrogenated $B_{10}C_{2+x}H_y$, these data can be used to determine N_a. Fitting these data to the $1/C^2$ form of Eq. (2) allows determination of N_a from the slope and V_i from the voltage intercept at $1/C^2 = 0$. Using values of $11.9 \times (8.854 \times 10^{-12})$ F/m and $3.5 \times (8.854 \times 10^{-12})$ F/m [18] for ε_n and ε_p, respectively and $N_d = 4.5 \times 10^{19}\,m^{-3}$, the carrier density for amorphous-$B_{10}C_{2+x}H_y$ (N_a) and the built in potential are obtained and presented in Fig. 4.

From Fig. 4a we find that for the virgin sample, the carrier concentration was $1.36 \times 10^{14}\,cm^{-3}$. The carrier concentration drops slightly after 10 h of irradiation (2.7×10^8 neutrons/cm^2) to $7.06 \times 10^{13}\,cm^{-3}$. There is a further drop in carrier concentration to $1.54 \times 10^{13}\,cm^{-3}$ after 20 h of irradiation (5.4×10^8 neutrons/cm^2). This is followed by another slight drop to $1.22 \times 10^{13}\,cm^{-3}$ after 40 h of irradiation (10.8×10^8 neutrons/cm^2). Similarly, the built-in potential also decreases with neutron irradiation. The built-in potential for the un-irradiated diode is 1.49 V, which decreases to 1.31 V after 10 h of neutron exposure, which further decreases to 0.83 V after 20 h, and finally decreases to 0.45 V after 40 h. The correlation between V_i and N_a is not surprising given that V_i is proportional to $\ln(N_a)$ [19]. A reduction in the charge carrier concentration means a smaller device built-in potential. A decrease in carrier concentration with neutron irradiation suggests that the number of defect states in the band gap of amorphous-$B_{10}C_{2+x}H_y$ has decreased.

Justification for assuming that the major changes taking place during neutron irradiation are occurring in amorphous-$B_{10}C_{2+x}H_y$, and not in the Si is supported by the HRTEM data and RBS channeling data presented in Figs. 5 and 6.

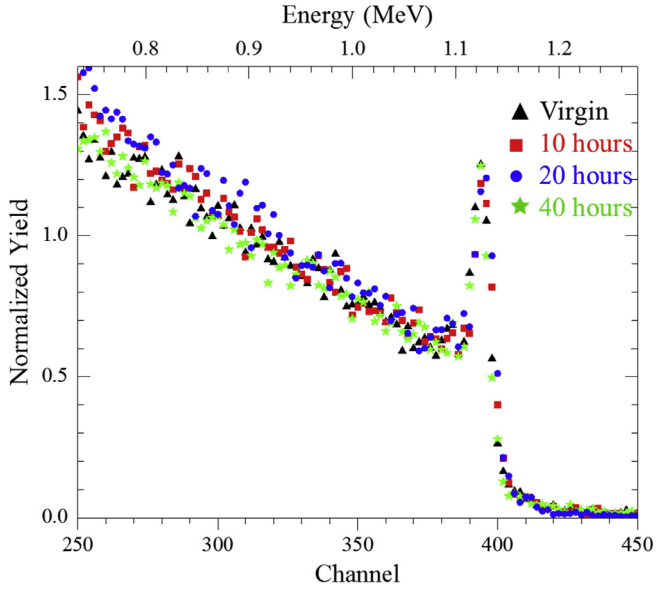

Fig. 6. Channeling spectra from Si portion of the a-$B_{10}C_{2+}$xHy/Si (p-n) diode following neutron irradiation and stripping the a-$B_{10}C_{2+x}H_y$ layer following neutron fluences of zero, 2.7×10^8, 5.4×10^8, and 10.8×10^8 neutrons/cm^2; i.e. 0 (virgin), 10, 20, and 40 h of exposure, respectively.

Table 1
Simulated projected range and energy loss for 0.84 MeV ^{7}Li and 1.27 MeV He^+ ions in a-$B_{10}C_{2+x}H_y$ (BC) and Si.

0.84 MeV Li	R_p (microns)	$dE/dx\|_n$ (eV/nm)	$dE/dx\|_e$(eV/nm)
BC	2.40	1.50	580.00
Si	2.46	1.80	487.00
1.47 MeV He	R_p (microns)	$dE/dx\|_n$(eV/nm)	$dE/dx\|_e$(eV/nm)
BC	4.60	0.26	296.30
Si	5.15	0.31	267.0

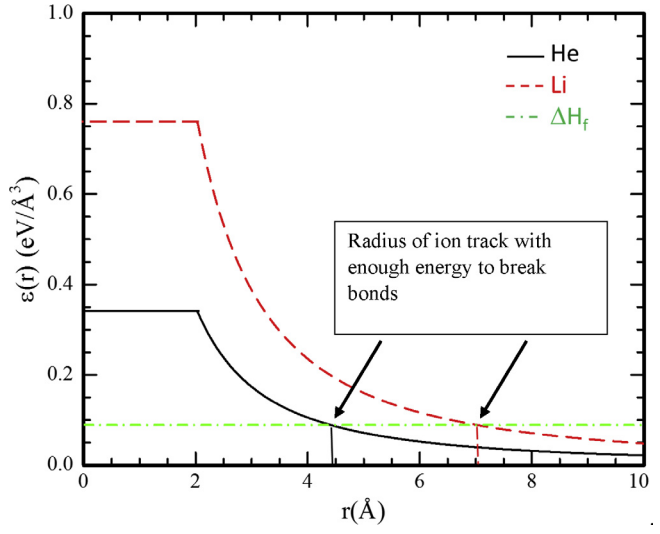

Fig. 7. Electronic energy density deposition in a-$B_{10}C_{2+x}H_y$ from 0.84 MeV Li and 1.27 MeV He ions. Also shown is the boron carbide heat of formation, which represent the energy threshold for bond breaking.

In an effort to identify changes in the device as a function of irradiation, HRTEM images and SAED patterns were obtained at the a-$B_{10}C_{2+x}H_y$/Si, interface and in the bulk Si far from the interface (200 nm and 800 nm), but still within the ^{7}Li and He^+ ion range after neutron capture/fragmentation in the a $B_{10}C_{2+x}H_y$, Fig. 5. These images show that the a-$B_{10}C_{2+x}H_y$ remains amorphous following 40 h of neutron irradiation (10.8×10^8 neutrons/cm^2), Fig. 5a, and that the junction interface remains abrupt, Fig. 5b. Finally, no discernible damage is apparent in the Si HTREM images or the SAED patterns, both near and far from the interface, Fig. 5c and d. However, point defects in Si are undetectable with this technique until they occur in concentrations high enough that point defect agglomeration begins to occur [11].

Rutherford backscattering spectrometry in channeling mode (RBS/C) was performed to examine damage development in the Si component of the a-$B_{10}C_{2+x}H_y$/Si diode. Previous research has shown that when the principle interaction between the channeling ion and the lattice defect is direct scattering (i.e., low densities of point defects and small defect clusters), RBS/C is more sensitive at detecting these defects relative to TEM [20]. Following exposure to neutrons, the surface layer of a-$B_{10}C_{2+x}H_y$ was fully stripped from the Si by submerging the diode in chromium etchant (Sigma Aldrich) for 24 h. Removal of a-$B_{10}C_{2+x}H_y$ allows for accurate channeling experiments to be performed on the Si. Fig. 6 shows the RBS/C spectra after exposure to neutron fluences of zero, 2.7×10^8, 5.4×10^8, and 10.8×10^8 neutrons/cm^2; i.e. zero exposure (virgin), 10, 20, and 40 h of exposure, respectively. These data show that within the resolution of the RBS/C technique, there is no discernible dechanneling, suggesting damage build up in the Si was negligible. These data, together with the TEM data presented in Fig. 5, show that the electrical property changes observed in Figs. 1–4 are most probably due to irradiation induced changes in the a-$B_{10}C_{2+x}H_y$. This conclusion is in agreement with our previous findings that device improvement as a result of irradiation is not due to changes in the interface, or changes in structure of the crystalline material. Instead, our supposition remains that the improvement is due to defect passivation of the amorphous boron carbide material.

Defect passivation of the a-$B_{10}C_{2+x}H_y$ by the passage of energetic ^{7}Li and He^+ ions can be argued from an energy deposition standpoint. Projected range, R_p, and energy loss, dE/dx, values for 0.84 MeV ^{7}Li and 1.27 MeV He^+ ions in a-$B_{10}C_{2+x}H_y$ and Si were calculated by the Monte Carlo simulation Stopping and Range of Ions in Matter (SRIM) code [21] and are presented in Table 1. As can be seen from examining these data, the dominant energy loss mechanism in the boron carbide, from the 0.84 MeV ^{7}Li and 1.27 MeV He^+ ions, is electronic energy loss, $dE/dx|_e$. A comparison of the energy deposition density along an ion track to the bond breaking energy can be made on the basis of estimates for the electronic stopping and the heat of formation for boron carbide. Domalski and Armstrong [22] experimentally determined the heat of formation, ΔH_f, of $B_{4.222}C$ to be -17.1 kcal/mol. Taking the atomic density of a-$B_{10}C_{2+x}H_y$ to be 12.0×10^{22} atoms/cm^3 the heat of formation can be recast as 0.089 eV/Å^3. This is essentially the energy density needed to break bonds in the boron carbide. We can equate this to the energy density deposited in an energetic ion track. Following Watson and Tombrello [23], we can calculate the energy deposition radial distribution for the ^{7}Li and He^+ ions, Fig. 7.

Fig. 7 shows the energy density of the electronic energy deposition, ε(r), as a function of track radius, r, for He^+ and ^{7}Li ions irradiating a-$B_{10}C_{2+x}H_y$. Also shown is the boron carbide heat of formation, which intersect the energy density curves at r equals 4.40 Å and 7.00 Å for the He^+ and ^{7}Li ions, respectively. These cut off values represent the radius of the ion track, below which sufficient energy is deposited to break bonds. As can be seen, the deposited energy is initially localized to approximately the first 2 Å of the ion track, and then falls off exponentially. These data show that sufficient energy is being deposited in a-$B_{10}C_{2+x}H_y$ to break bonds, which can reform in different configurations during energy dissipation. During bond reformation, repair of bond defects that originate during the plasma enhanced chemical vapor deposition process can take place, which can result in defect passivation and improvement in electrical properties.

The n-type plasma enhanced chemical vapor deposition (PECVD) boron carbide on p-type silicon heterojunctions behave much

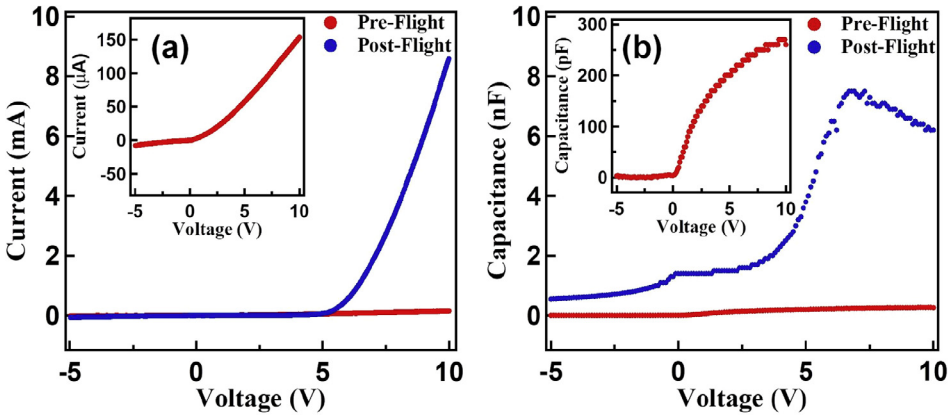

Fig. 8. The transport I(V) and C(V) measurements on PECVD (n-type) boron carbide films derived from the metacarborane precursor on p-type silicon. (a) I-V data for Pre-Flight (red curve) and Post-Flight (blue curve) (b) C-V data for Pre-Flight (red curve) and Post-Flight (blue curve). Notice that Post-Flight data shows marked improvement compared to the Pre-Flight measurements in both I-V and C-V data. (For interpretation of the references to colour in this figure legend, the reader is referred to the web version of this article.)

differently than the diodes discussed above. This is in part because the diodes are very dielectric prior to radiation exposure with very little forward bias current, as seen in Fig. 8, although there is very clear evidence for rectification. These samples were exposed to the radiation hard environment of low earth orbit for roughly 2.2×10^3 h (total solar exposure), aboard the International Space Station, on the zenith side, encountering no less than 1500 neutrons and ionizing radiation (in part due to a high background proton flux) per cm^2second. The changes in the reverse bias current are very small, indicative of a huge improvement in diode performance, if the figure-of-merit is forward bias current versus reverse bias current, as seen in Fig. 8. This tends to point to a mechanism for the evolution of the semiconductor in that the carrier concentration increases with radiation exposure, rather than decreases. In general though, if radiation results in creation of electron carriers, then the p-type PECVD boron carbide semiconductor will have the potential for charge compensation, resulting in an effective decrease in the combined carrier concentration if the electron – hole pairs either recombine or trap, possibly as a tightly bound exciton or bi-polaron, as has been suggested [24].

4. Conclusion

In conclusion, heterojunction diodes of amorphous partially dehydrogenated p-type semiconducting boron carbide, synthesized via PECVD on n-type single crystal silicon were exposed to thermal neutrons for up to 40 h (10.8×10^8 neutrons/cm^2). This research provides evidence that the electrical properties of amorphous partially dehydrogenated semiconducting boron carbide on silicon p-n heterojunction diodes initially improve with neutron irradiation, contrary to nearly all traditional electronic devices. The cause for the device improvement is most likely a result of a defect passivation within the a-$B_{10}C_{2+x}H_y$ component of the diode, which interestingly leads to a decrease of carrier concentration with radiation exposure. Further, there is a direct correlation between the trends of the carrier concentration, built-in potential of the diode, and as shown previously, the drift carrier lifetimes. In contrast, the dramatic improvement in device performance for n-type plasma enhanced chemical vapor deposition (PECVD) hydrogenated semiconducting boron carbide on p-type silicon, suggests an increased carrier concentration with radiation exposure. We find, nonetheless, that heterojunction diodes of partially dehydrogenated n-type semiconducting boron carbide, synthesized via PECVD on p-type single crystal silicon, shows significant improvements upon exposure to radiation.

This research indicates that some disorder within the amorphous semiconductor film (in the form of defects) undergoes healing with irradiation. This increases the operational lifetime of the device. Perhaps more importantly, this research provides further evidence that future devices would benefit from a fully amorphous diode composed of n and p type a-$B_{10}C_{2+x}H_y$.

Acknowledgements

This work was supported by the Office of Research and Economic Developmentat the University of Nebraska-Lincoln, the Defense Threat Reduction Agency(Grant No. HDTRA1-14-1-0041), and the Office of Naval Research (Contracts #FA4600-12-D-9000-0045 and #FA4600-12-D-9000-0057). This work was performed, in part, at the Center for Integrated Nanotechnologies, an Office of Science User Facility operated for the U.S. Department of Energy (DOE) Office of Science. Los Alamos National Laboratory, an affirmative action equal opportunity employer, is operated by Los Alamos National Security, LLC, for the National Nuclear Security Administration of the U.S. Department of Energy under contract DE-AC52-06NA25396. The work was carried out in part in the Central Facilities of the Nebraska Center for Materials and Nanoscience, which is supported by the Nebraska Research Initiative. The authors would like to acknowledge S. Ducharme of the Department of Physics and Astronomy at the University of Nebraska – Lincoln for allowing the use of his laboratory's impedance analyzer. The authors would like to acknowledge S. Adenwalla of the Department of Physics and Astronomy at the University of Nebraska – Lincoln for allowing the use of her laboratory's neutron generator which was funded in part by the Office of Research and Economic Development (ORED). The authors thank Ethiyal Wilson for his technical assistance with the preliminary measurements of the n-type boron carbide to p-type silicon heterojunction diodes.

References

[1] B.W. Robertson, S. Adenwalla, A. Harken, P. Welsch, J.I. Brand, P.A. Dowben, J.P. Claassen, A class of boron-rich solid-state neutron detectors, Appl. Phys. Lett. 80 (2002) 3644–3646.
[2] A.N. Caruso, P.A. Dowben, S. Balkir, N. Schemm, K. Osberg, R.W. Fairchild, O.B. Flores, S. Balaz, A.D. Harken, B.W. Robertson, J.I. Brand, The all boron carbide diode neutron detector: Comparison with theory, Mat. Sci. Eng. B-Solid 135 (2006) 129–133.
[3] A.N. Caruso, The physics of solid-state neutron detector materials and geometries, J. Phys.-Condens. Mat. 22 (2010).
[4] S. Adenwalla, R. Billa, J.I. Brand, E. Day, M.J. Diaz, A. Harken, A. McMullen-Gunn, R. Padmanabhan, B.W. Robertson, Semiconducting boron-rich neutron detectors, Proc. SPIE (2004) 70–74.
[5] N.N. Hong, J. Mullins, K. Foreman, S. Adenwalla, Boron carbide based solid state neutron detectors: the effects of bias and time constant on detection efficiency, J. Phys. D Appl. Phys. 43 (2010).
[6] N. Hong, L. Crow, S. Adenwalla, Time-of-flight neutron detection using PECVD grown boron carbide diode detector, Nucl. Instrum. Methods Phys. Res., Sect. A 708 (2013) 19–23.
[7] E. Echeverria, R. James, U. Chiluwal, F.L. Pasquale, J.A.C. Santana, R. Gapfizi, J.D. Tae, M.S. Driver, A. Enders, J.A. Kelber, P.A. Dowben, Novel semiconducting boron carbide/pyridine polymers for neutron detection at zero bias, Appl. Phys. a-Mater. 118 (2015) 113–118.
[8] E. Echeverría, R. James, F.L. Pasquale, J.A. Colón Santana, M.S. Driver, A. Enders, K.J. A, P. Dowben, Neutron detection signatures at zero bias in novel semiconducting boron carbide/pyridine polymers, MRS Proc. 1743 (2015).
[9] G.F. Knoll, Radiation Detection and Measurement, third ed., Wiley, New York, 2000.

[10] M. Nastasi, J.W. Mayer, J.K. Hirvonen, Ion-Solid Interactions: Fundamentals and Applications, Cambridge University Press, Cambridge, 1996.
[11] G. Peterson, Q. Su, Y. Wang, P.A. Dowben, M. Nastasi, Improved p-n heterojunction device performance induced by irradiation in amorphous boron carbide films, Mater. Sci. Eng. B-Adv. 202 (2015) 25–30.
[12] B.W. Robertson, S. Adenwalla, A. Harken, P. Welsch, J.I. Brand, J.P. Claassen, N.M. Boag, P.A. Dowben, Semiconducting boron-rich neutron detectors, Proc. SPIE (2002) 226–233.
[13] E. Echeverria, B. Dong, A.Y. Liu, E.R. Wilson, G. Peterson, M. Nastasi, P.A. Dowben, J.A. Kelber, Strong binding at the gold (Au) boron carbide interface, Surf. Coat Tech. 314 (2017) 51–54.
[14] C. Höglund, K. Zeitelhack, P. Kudejova, J. Jensen, G. Greczynski, J. Lu, L. Hultman, J. Birch, R. Hall-Wilton, Stability of $^{10}B_4C$ thin films under neutron radiation, Radiat. Phys. Chem. 113 (2015) 14–19.
[15] S. Lee, J. Mazurowski, G. Ramseyer, P.A. Dowben, Characterization of boron-carbide thin-films fabricated by plasma enhanced chemical vapor-deposition from boranes, J. Appl. Phys. 72 (1992) 4925–4933.
[16] G.W. Neudeck, The PN Junction Diode, second ed., Addison-Wesley Publishing Company, 1989.
[17] R.L. Anderson, Experiments on Ge-gaas heterojunctions, Solid State Electron. 5 (1962) 341.
[18] G. Peterson, Electrical Characterization of Irradiated Semiconducting Amorphous Hydrogenated Boron Carbide, University of Nebraska-Lincoln, 2017.
[19] http://ecee.colorado.edu/~bart/book/book/copyrigh.htm.
[20] K. Yasuda, M. Nastasi, K.E. Sickafus, C.J. Maggiore, N. Yu, Ion beam channeling study on the damage accumulation in yttria-stabilized cubic zirconia, Nucl. Instrum. Methods B 136 (1998) 499–504.
[21] J.F. Ziegler, J.P. Biersack, U. Littmark, The Stopping and Range of Ions in Solids, Pergamon Press, New York, 1985.
[22] E.S. Domalski, G.T. Armstrong, The heat of formation of boron carbide, Journal of Research of the National Bureau of Standards-A, Phys. Chem. 72A (1968) 133.
[23] C.C. Watson, T.A. Tombrello, A modified lattice potential model of electronically mediated sputtering, Radiat. Eff. Defects Solids 89 (1985) 263.
[24] O. Chauvet, D. Emin, L. Forro, T.L. Aselage, L. Zuppiroli, Spin susceptibility of boron carbides: dissociation of singlet small bipolarons, Phys. Rev. B 53 (1996) 14450–14457.